All Digital Frequency Synthesis Based on Pulse Direct Digital Synthesizer with Spurs Free Output and Improved Noise Floor

Paul P. Sotiriadis
Department of Electrical and Computer Science
National Technical University of Athens
Athens, Greece
E-mail: pps@ieee.org

***Abstract*—This work presents Direct-Digital Frequency Synthesis architectures based on the classical Pulse-Direct Digital Synthesizer and using two quantization paths with opposite dithers or multi-path quantization with independent dithers to achieve spurs-free output with improved dynamic range. The proposed architectures are studied mathematically and the theory is supported by MATLAB simulation results.**

Keywords—Dithering, Direct digital synthesis, frequency spurs, noise shaping, quantization, spectrum

I. Introduction

All-digital architectures have attracted the interest of the scientific community over the past few years [1]-[4]. This is motivated by the increasing challenges in the design of classical analog blocks as integration technologies down-scale to a few tens of nano-meters. Digital circuits instead, offer the robustness to noise, temperature, power supply and process variations, as well as the advantages of design automation. Research in all-digital frequency synthesis can be traced at least three decades back [5]-[7].

Frequency synthesis is a critical and usually challenging part of RF circuit design. It has followed the trend of digitally intensive design resulting in two main classes of circuits: the All-Digital Phase-Locked Loops (ADPLL) [1] and the Direct Digital Synthesizers (DDS) [8]. Although both have led to many successful products, they both still have analog and/or mixed-signal blocks that need to be designed carefully for the technology the I.C. is to be fabricated.

Efforts have been made to remove the DAC, the only mixed-signal block, in DDS leading to Pulse-DDS (PDDS) [5],[9],[10]. This however introduces the challenging task of generating single-bit digital signals of desirable sinewave-like spectrum using only the reference clock [6],[9][2]. Unless the generated frequency is an integer fraction of the clock, their output waveforms are irregular with high deterministic jitter and spectra full of strong frequency spurs, usually close to the carrier. This inherent problem of such architectures creates the need for additional techniques to suppress the frequency spurs (or to reduce the deterministic jitter). The only purely digital method to do so is using (random) dithering [9].

It has been shown that in PDDS, random dithering of appropriate statistics leads to spurs-free output [10]-[12]. However, dithering results in raised noise floor. If one can tolerate the presence of some spurious frequency components, it is possible that the random dithering can be modified to get a small improvement in the noise floor [13].

This paper presents two variations of the dithered PDDS [10], one with two quantization paths with opposite dithering and one general class of multi-path quantization with independent dithers. Both schemes are analyzed mathematically to derive their output spectra and dynamic ranges. The improvements in their noise floor are derived with respect to the basic, dithered, spurs-free PDDS [10].

II. Definitions and Basic Facts

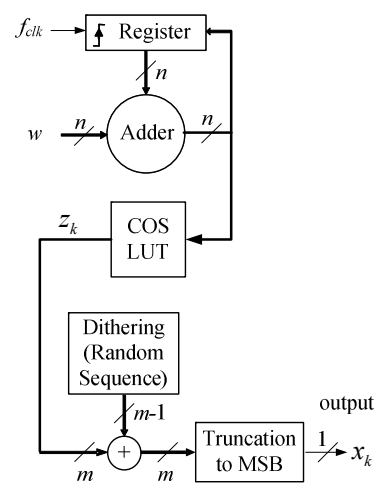

Fig. 1: Pulse Direct Digital Synthesizer (PDDS) with amplitude dithering (random sequence).

The structure of PDDS with amplitude dithering [10] is shown in Fig. 1. It consists of an n-Bit phase accumulator generating $kw \bmod 2^n$ (where k is the clock pulse counter) driving a sinusoidal Look-Up-Table (LUT). The m-Bit output of the LUT is a quantized version of the sinusoidal $z_k = \left(\cos\left(\Omega k\right)+1\right)/2$ where $\Omega = 2\pi w / 2^n$ with $w < 2^{n-1}$.

The *Dithering* block uses a Random Number Generator to generate the sequence $\{r_k / 2^m\}$ of pseudo-random, (ideally) independent and uniformly distributed in $\{0,1,2,...,2^m-1\}$ random numbers r_k, $k=0,1,2,...$. Finally, the sum $z_k + r_k / 2^m$ is truncated to its MSB.

The crude MSB quantization at the output is far more important in spurs (and noise when dithered) generation than the quantization error in the representation of the sinusoidal by the LUT as well as the quantization error of the representation of the dithering (e.g for $m \geq 8$). To this end, the output of the dithered PDDS can be shown to be practically equivalent to that of the scheme in Fig. 2 [10],[11].

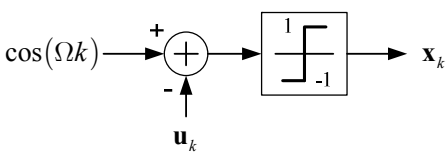

Fig. 2: Dithered 1-Bit quantized sinewave capturing PDDS' behavior

Without any loss, in Fig. 2 we consider ± 1 output and an Independent and Identically Distributed (IID) random dither $\{\mathbf{u}_k\}$ which is uniformly distributed in $[-1,1]$. The output is

$$\mathbf{x}_k = \mathrm{sgn}\left(\cos(\Omega k) - \mathbf{u}_k\right) \tag{1}$$

which can be expressed as

$$\mathbf{x}_k = \begin{cases} 1 & \text{if } \mathbf{u}_k < \cos(\Omega k) \\ -1 & \text{if } \mathbf{u}_k > \cos(\Omega k) \\ 0 & \text{otherwise} \end{cases}$$

Considering $\cos(\Omega k)$ as the desirable output, the output error $\mathbf{e}_k$ is defined by

$$\mathbf{x}_k = \cos(\Omega k) + \mathbf{e}_k \,. \tag{2}$$

It has been shown that the output $\mathbf{x}_k$, and therefore that of the PDDS, assuming sufficient resolution of the LUT and the RNG, is spurs-free with a flat noise floor [11] of discrete-time PSD $s_{\mathbf{e}}(\omega) = 1/2$. The situation is illustrated in Fig. 3. Also, for sampling frequency f_S, the output has Dynamical Range [11],[12]

$$DR = 10\log_{10}(f_S) - 3.01 \quad \text{(dB)} \tag{3}$$

where *DR* is defined as the power of the desirable signal, at frequency $f = \Omega \cdot f_S / (2\pi)$, over the power spectral density of the noise floor near it (for the continuous-time signals). Note that the dynamic range observed on the spectrum analyzer (simulation here) is $10\log_{10}(RBW)$ dB below *DR* due to the resolution bandwidth *RBW* of the measurement.

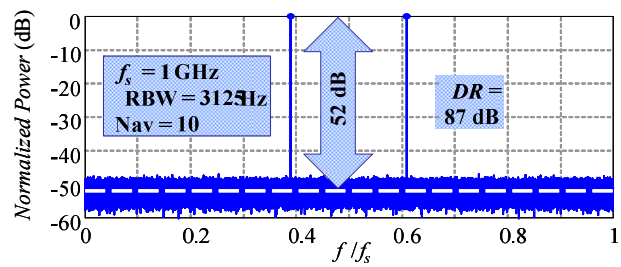

Fig. 3: PSD of dithered PDDS when $w=25$, $n=6$, $f_S = 1\,GHz$, resolution bandwidth BW = 3125 Hz, and waveform averaging is 10

A. Basic Facts

Here we introduce some basic facts that will be used to simplify the derivations in the following sections. Consider the scheme in Fig. 4 where we have used v instead of $\cos(\Omega k)$ as the input.

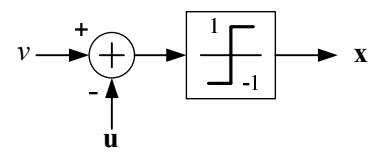

Figure 4: Dithered quantization of a fixed number v

We assume that $v \in [-1,1]$ and $\mathbf{u}$ is a random variable uniformly distributed in $[-1,1]$. Since $\mathbf{x} = \mathrm{sgn}(v - \mathbf{u})$ we have directly that $\mathbf{x} \in \{\pm 1\}$ (note that the probability of $\mathbf{x} = 0$ is zero and is ignored) and that for every $v \in [-1,1]$ it is $\Pr(\mathbf{x}=1) = (1+v)/2$ and $\Pr(\mathbf{x}=-1) = (1-v)/2$. They imply directly that $E\{\mathbf{x}\} = \Pr(\mathbf{x}=1) - \Pr(\mathbf{x}=-1) = v$ and so $E\{\mathbf{e}\} = 0$ for the output quantization error $\mathbf{e} = \mathbf{x} - v$. Moreover $E\{\mathbf{e}v\} = 0$ and the variation (power) of the error is $E\{\mathbf{e}^2\} = E\{\mathbf{x}^2 - 2\mathbf{x}v + v^2\} = 1 - v^2$. Summarizing:

$$E\{\mathbf{x}\} = v\,,\; E\{\mathbf{e}\} = 0\,,\; E\{\mathbf{e}v\} = 0\,,\; E\{\mathbf{e}^2\} = 1 - v^2\,. \tag{4}$$

B. Power Spectral Density of Non Wide-Sense Stationary Random Sequences

When a random sequence $\{\mathbf{y}_k\}$ is Wide-Sense Stationary (WSS), its Power Spectral Density (PSD) is defined as the Discrete-Time Fourier Transform (DTFT) of its autocorrelation function [14], $r_{\mathbf{y}}(k) = E\{\mathbf{y}_{m+k}\mathbf{y}_m\}$ which is independent of the time m. Here, from Eq. (1) we note that the output and error random sequences, $\{\mathbf{x}_k\}$ and $\{\mathbf{e}_k\}$, are not WSS because they depend on $\cos(\Omega k)$ and therefore on the discrete time k. The autocorrelation function of $\{\mathbf{x}_k\}$ is

$$r_{\mathbf{x}}(n,m) = E\{\mathbf{x}_n \mathbf{x}_m\}\,.$$

To define the PSD of $\{\mathbf{x}_k\}$, instead of $r_{\mathbf{x}}(n,m)$ we can use the time-average autocorrelation function [15]

$$\overline{r}_{\mathbf{x}}(k) \triangleq \lim_{M\to\infty} \frac{1}{2M+1} \sum_{m=-M}^{M} r_{\mathbf{x}}(k+m,m)$$

which is well defined for a wide class of random sequences $\{\mathbf{x}_k\}$ in general. To simplify notation, we use $\overline{r_{\mathbf{x}}(k+m,m)}^{m}$ to indicate the time-averaging with respect to variable m. Then, the PSD of output $\{\mathbf{x}_k\}$ is the DTFT of $\{\overline{r}_{\mathbf{x}}(k)\}$, i.e.,

$$s_{\mathbf{x}}(\omega) = \sum_{k=-\infty}^{\infty} \overline{r}_{\mathbf{x}}(k) e^{-ik\omega}.$$

The definitions above are applicable to the variations of output sequence $\{\mathbf{x}_k\}$ generated by the schemes in the following sections.

III. Two Quantizers with Opposite Dithers

One way to reduce the noise level is to use two single-bit quantizers with opposite dithers, and, average their outputs as it is illustrated in Fig. 5 below.

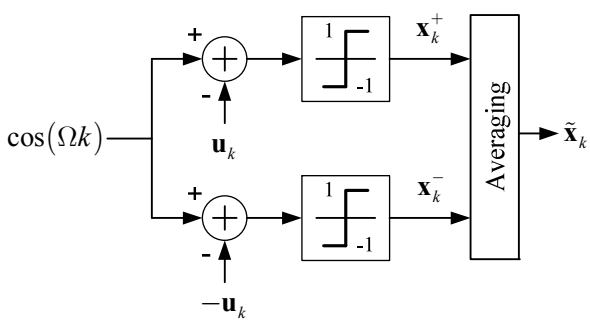

Fig. 5: Averaging the outputs of two PDDS with opposite dithers

Since $\mathbf{x}_k^{\pm} = \operatorname{sgn}(\cos(\Omega k) \mp \mathbf{u}_k)$ the output is

$$\tilde{\mathbf{x}}_k = \frac{1}{2}\left[\operatorname{sgn}(\cos(\Omega k) - \mathbf{u}_k) + \operatorname{sgn}(\cos(\Omega k) + \mathbf{u}_k)\right]. \quad (5)$$

It is straightforward to verify that

$$\tilde{\mathbf{x}}_k = \begin{cases} \operatorname{sgn}(\cos(\Omega k)) & \text{if } |\mathbf{u}_k| < |\cos(\Omega k)| \\ 0 & \text{otherwise} \end{cases} \quad (6)$$

Since both $\pm\mathbf{u}_k$ are uniformly distributed in $[-1,1]$, using (4) and (5) we derive directly that

$$E\{\tilde{\mathbf{x}}_k\} = \cos(\Omega k). \quad (7)$$

Note also that for every $m \neq n$, $\mathbf{u}_n, \mathbf{u}_m$ are independent and so $\tilde{\mathbf{x}}_n, \tilde{\mathbf{x}}_m$ are independent to each other too. Therefore

$$\begin{aligned} r_{\tilde{\mathbf{x}}}(n,m) &= E\{\tilde{\mathbf{x}}_n \tilde{\mathbf{x}}_m\} \\ &= E\{\tilde{\mathbf{x}}_n\} E\{\tilde{\mathbf{x}}_m\} \\ &= \cos(\Omega n)\cos(\Omega m) \\ &= \frac{1}{2}\cos(\Omega(n-m)) + \frac{1}{2}\cos(\Omega(n+m)) \end{aligned}.$$

and setting $n = m+k$ with $k \neq 0$,

$$r_{\tilde{\mathbf{x}}}(m+k,m) = \frac{1}{2}\cos(\Omega k) + \frac{1}{2}\cos(\Omega(2m+k)).$$

The time-average autocorrelation function of $\{\tilde{\mathbf{x}}_k\}$ is

$$\begin{aligned} \overline{r}_{\tilde{\mathbf{x}}}(k) &= \overline{r_{\tilde{\mathbf{x}}}(k+m,m)}^{m} \\ &= \lim_{M\to\infty} \frac{1}{2M+1} \sum_{m=-M}^{M} r_{\tilde{\mathbf{x}}}(m+k,m) \\ &= \frac{1}{2}\cos(\Omega k) + \overline{\cos(\Omega(2m+k))}^{m} \\ &= \frac{1}{2}\cos(\Omega k) \end{aligned}.$$

To derive $\overline{r}_{\tilde{\mathbf{x}}}(0)$ we start from $E\{\tilde{\mathbf{x}}_m^2\}$ and observe from (6) that $\tilde{\mathbf{x}}_m^2$ can be either 0 or 1. Since $\mathbf{u}_k$ is uniformly distributed in $[-1,1]$, again from Eq. (6) we get that $\Pr(\tilde{\mathbf{x}}_m^2 = 1) = |\cos(\Omega m)|$ for every m. We conclude that $E\{\tilde{\mathbf{x}}_m^2\} = |\cos(\Omega m)|$. Recalling that $\Omega = 2\pi w / 2^n$, it can be shown that the average value of $|\cos(\Omega m)|$, and therefore the value of $\overline{r}_{\tilde{\mathbf{x}}}(0)$ is

$$\overline{|\cos(\Omega m)|}^{m} = \begin{cases} \dfrac{\sin(2\pi/2^r)}{2^{r-1}\left[1-\cos(2\pi/2^r)\right]} & \text{if } r \geq 2 \\ 1 & \text{otherwise} \end{cases}$$

where $r = n - \log_2(\gcd(2^n, w))$. Note that it is $w < 2^{n-1}$ by assumption and so it is always $r \geq 2$. Moreover $r = 2$ is possible only for $w = 2^{n-2}$, i.e. when the scheme operates as an integer divider by 4. It can be verified that

$$\overline{|\cos(\Omega m)|}^{m} = \begin{cases} 1/2 & \text{if } r = 2 \\ \cong 2/\pi & \text{otherwise} \end{cases}$$

Finally, the complete form of $\overline{r}_{\tilde{\mathbf{x}}}(k)$ is

$$\overline{r}_{\tilde{\mathbf{x}}}(k) = \frac{1}{2}\cos(\Omega k) + \left(\overline{|\cos(\Omega m)|}^{m} - \frac{1}{2}\right)\delta_k. \quad (8)$$

Ideally, one would like to have an output identical to the input $\cos(\Omega k)$. We set $v_k = \cos(\Omega k)$ and calculate the

PSD of it in a form compatible with that of the random output $\tilde{\mathbf{x}}_k$ [15], i.e., as the DTFT of $\overline{r}_v(k)$ where

$$\overline{r}_v(k) = \overline{\cos(\Omega(m+k))\cos(\Omega m)}^m = \frac{1}{2}\cos(\Omega k). \quad (9)$$

We define the error $\tilde{\mathbf{e}}_k$ similarly to Eq. (2) via

$$\tilde{\mathbf{x}}_k = v_k + \tilde{\mathbf{e}}_k$$

and note that $E\{\tilde{\mathbf{e}}_n v_m\} = 0$ for every n, m from Eq. (4). Therefore we have

$$\overline{r}_{\tilde{\mathbf{x}}}(k) = \overline{r}_v(k) + \overline{r}_{\tilde{\mathbf{e}}}(k) \quad (10)$$

and taking the DTFT of it,

$$s_{\tilde{\mathbf{x}}}(\omega) = s_v(\omega) + s_{\tilde{\mathbf{e}}}(\omega).$$

Eqs. (8), (9) and (10) imply $\overline{r}_{\tilde{\mathbf{e}}}(k) = \left(\overline{|\cos(\Omega m)|}^m - \frac{1}{2}\right)\delta_k$ and taking the DTFT of it we get

$$s_{\tilde{\mathbf{e}}}(\omega) = \overline{|\cos(\Omega m)|}^m - \frac{1}{2}$$

which for $w \neq 2^{n-2}$ can be approximated by

$$s_{\tilde{\mathbf{e}}}(\omega) \cong \left(\frac{2}{\pi} - \frac{1}{2}\right)\delta_k \cong 0.137 \cdot \delta_k. \quad (11)$$

A. Output Dynamic Range

Let the sampling frequency be f_s and convert the PSD of the desirable signal $v_k = \cos(\Omega k)$ and that of the error $\tilde{\mathbf{e}}_k$ to the continuous-time domain. It can be seen that [11]

$$S_v(f) = \frac{W(f)}{4}\sum_{k=-\infty}^{\infty}\delta\left(f - kf_s \mp \frac{\Omega}{2\pi}f_s\right) \quad (12)$$

and

$$S_{\tilde{\mathbf{e}}}(f) = \frac{W(f)}{f_s}\left(\overline{|\cos(\Omega m)|}^m - \frac{1}{2}\right)$$

respectively, where $W(f)$ is the pulse-shape factor of the output; for digital ± 1 output signal, $W(f) = \mathrm{sinc}^2(fT_S)$. Then the Dynamic Range of the output is defined as the ratio of the power of the signal at the frequency $\frac{\Omega}{2\pi}f_s$ over the power spectral density of the noise near it, as in [11]-[13]. Therefore we have

$$DR = 10\log_{10}\left(\frac{f_s}{4\left(\overline{|\cos(\Omega m)|}^m - \frac{1}{2}\right)}\right) \text{ (dB)}$$

Assuming $w \neq 2^{n-2}$ and using Eq. (11) we conclude that

$$DR = 10\log_{10}(f_s) + 2.61 \quad \text{(dB)}$$

To take into account the resolution bandwidth, *RBW*, of the spectrum analyzer we observe the signal we need to subtract $10\log_{10}(RBW)$ and so what we observe is

$$DR_O = 10\log_{10}(f_s) - 10\log_{10}(RBW) + 2.61 \text{ (dB)} \quad (13)$$

An example spectrum is shown in Fig. 6 for $w = 25$, $n = 6$ and with simulation parameters $f_s = 1GHz$ and *RBW*=3125Hz. From Eq. (13) we get DR_O= 57.66 dB which is verified by the estimate of the average noise-floor near the desirable signal. There is an improvement of approximately 5.7 dB in noise floor compared to the output of the simple PDDS shown in Fig.3.

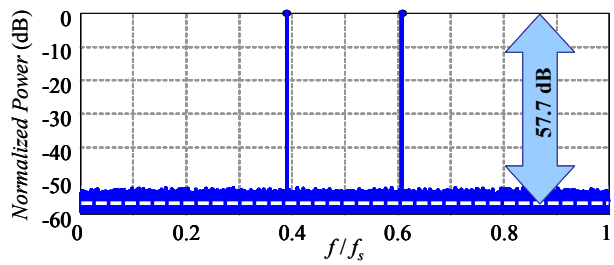

Fig. 6: PSD of dithered PDDS when $w = 25$, $n = 6$, $f_S = 1\,GHz$, resolution bandwidth RBW = 3125 Hz, and waveform averaging is 10

IV. MULTIPLE QUANTIZERS WITH INDEPENDENT DITHERING SEQUENCES

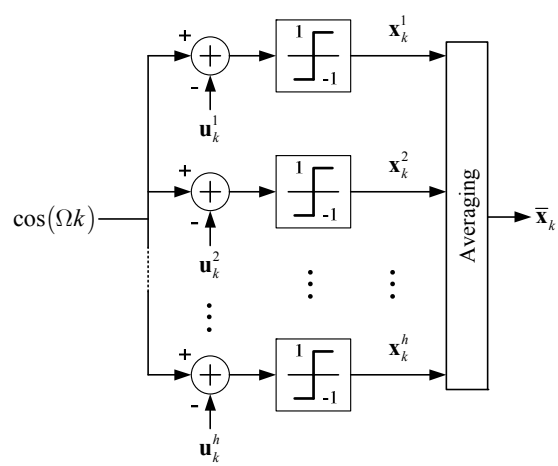

Fig. 7: Multi-path PDDS with independent dithers

It is worth mentioning that using the opposite dithers in the previous section, results in lower noise floor that using two independently dithered paths and taking the average output. This last concept is generalized in Fig. 7 where a number of h paths is used, each with an IID uniformly distributed in $[-1,1]$ random sequence $\{\mathbf{u}_k^j\}$, $j=1,2,3,..,h$ and all sequences are independent of each other.

For $j=1,2,3,..,h$ it is $\mathbf{x}_k^j = \mathrm{sgn}\left(\cos(\Omega k) - \mathbf{u}_k^j\right)$ and we define the errors as before $\mathbf{x}_k^j = \cos(\Omega k) + \mathbf{e}_k^j$. The output is

$$\overline{\mathbf{x}}_k = \frac{1}{h}\sum_{j=1}^{h}\mathbf{x}_k^j = \cos(\Omega k) + \frac{1}{h}\sum_{j=1}^{h}\mathbf{e}_k^j .$$

Since the random dithers are independent to each other and have the same autocorrelation, the total time-average autocorrelation of the error is $1/h$ times that of the simple PDDS [11]. Therefore, considering the output in the continuous-time domain, the desirable output part of the spectrum is as in Eq. (12), while the noise PSD is

$$S_{\overline{\mathbf{e}}}(f) = \frac{W(f)}{2hf_s}. \tag{14}$$

A. Output Dynamic Range of the Multi-path PDDS

From Eqs. (12) and (14), the Dynamic Range of the output, defined as above [11], is

$$DR = 10\log_{10}(h \cdot f_s) - 3.01 \text{ (dB)}$$

i.e., we have an improvement of $10\log_{10}(h)$ dB with respect to the DR of the simple PDDS in Eq. (3), [11]. Taking into account the resolution bandwidth of the spectrum analyzer we conclude that

$$DR_O = 10\log_{10}(h \cdot f_s) - 10\log_{10}(RBW) - 3.01 \text{ (dB)}. \tag{15}$$

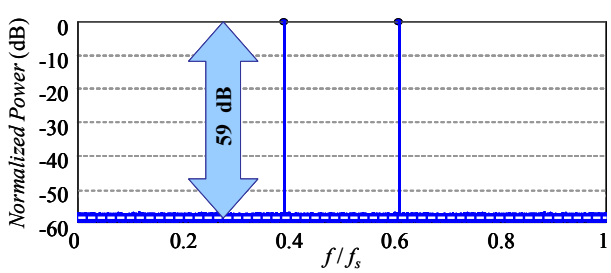

Fig. 8: PSD of multi-path dithered PDDS with $h=5$ when $w=25$, $n=6$, $f_s = 1\,GHz$, RBW = 3125 Hz, and waveform averaging is 150

The spectrum for $h=5$ paths is shown in Fig. 8. Again $w=25$, $n=6$ and simulation parameters are $f_s = 1GHz$ and RBW=3125Hz. From Eq. (15) we get DR_O=59 dB, which is verified by the numerical estimate of the average noise-floor near the desirable signal. There is an improvement of approximately 7 dB in noise floor compared to the output of the simple PDDS shown in Fig. 3.

V. Conclusions

This work has introduced two Direct-Digital Frequency Synthesis architectures based on the classical Pulse-Direct Digital Synthesizer. The first one has two single-bit quantization paths with opposite dithers and averaging at the output. The second one has multiple (h) single-bit quantization paths with independent dithers and averaging at the output. The proposed architectures were analyzed mathematically. They demonstrated 5.7 dB and $10\log_{10}(h)$ dB reduction in noise floor repetitively, relatively to the simple Pulse-Direct Digital Synthesizer with uniform dithering. The theory was supported by MATLAB simulation.

Acknowledgement

Described work was partially supported by Broadcom Foundation USA

References

[1] R. Staszewski, P. Balsara, All-Digital Frequency Synthesizer in Deep-Submicron CMOS, Wiley, 2006.

[2] H. Mair and L. Xiu, "An architecture of high-performance frequency and phase synthesis," IEEE J. Solid-State Circuits, vol. 35, no. 6, pp. 835–846, Jun. 2000.

[3] D. E. Calbaza and Y. Savaria, "A direct digital periodic synthesis circuit," IEEE J. Solid-State Circ., vol. 37, no. 8, pp. 1039–1045, 2002.

[4] E. Temporiti, C. Weltin-Wu, D. Baldi, R. Tonietto, F. Svelto, "A 3 GHz fractional all-digital PLL with a 1.8 MHz bandwidth implementing spur reduction techniques", IEEE JSSC 44(3), 824-834.

[5] V.S. Reinhardt, "Direct digital synthesizers", Technical Report, Hughes Aircraft Co, Space and Communications Group, L.A., CA, Dec. 1985.

[6] C. E. Wheatley, III, "Digital frequency synthesizer with random jittering for reducing discrete spectral spurs," U.S. Patent 4410954, Oct. 1983.

[7] V. N. Kochemasov and A. N. Fadeev, "Digital-computer synthesizers of two-level signals with phase-error compensation," Telecommun. Radio Eng., vol. 36/37, pp. 55–59, Oct. 1982.

[8] U.L. Rohde, *Microwave and Wireless Synthesizers: Theory and Design*, 1st ed. Singapore: Wiley-Interscience, 1997.

[9] P. Sotiriadis, K. Galanopoulos, "Direct All-Digital Frequency Synthesis Techniques, Spurs Suppression, and Deterministic Jitter Correction", IEEE Transactions on Circuits and Systems-I, Vol. 59, No. 5, May 2012, pp. 958-968.

[10] K. Galanopoulos, P. Sotiriadis, "Optimal Dithering Sequences for Spurs Suppression in Pulse Direct Digital Synthesizers", IEEE International Frequency Control Symposium 2012.

[11] P. Sotiriadis, N. Miliou, "Single-Bit Digital Frequency Synthesis via Dith-ered Nyquist-rate Sinewave Quantization", IEEE Trans. on Circuits and Systems-I. Vol. 61, No. 1, Jan. 2014, pp. 61-73.

[12] P. Sotiriadis, N. Stamatopoulos, "All-Digital Frequency Synthesis based on Single-Bit Nyquist-Rate Sinewave Quantization with IID Random Dithering", IEEE Int. Frequency Control Symposium 2013.

[13] P. Sotiriadis, N. Stamatopoulos, "Dynamic Range Vs Spectral Clarity Trade-off in All-Digital Frequency Synthesis via Single-Bit Sinewave Quantization", IEEE Int. Frequency Control Symposium 2013.

[14] A. Papoulis, S.U. Pillai, Probability, Random Variables and Random Processes, McGraw-Hill Europe; 4th Ed., 2002.

[15] L. Ljung, System Identification: Theory for the User 2nd Ed., Prentice Hall 1999.